

Time Variation in the Radio Flux Density from the Bipolar Ultracompact H II Region NGC 7538 IRS1

Ramiro Franco-Hernández and Luis F. Rodríguez

*Centro de Radioastronomía y Astrofísica, UNAM, Apdo. Postal 3-72 (Xangari), 58089
Morelia, Michoacán, México*

r.franco, l.rodriguez@astrosmo.unam.mx

ABSTRACT

We present high angular resolution ($\sim 0''.1$ - $0''.4$) VLA observations at 2 and 6 cm made in 1983, 1986, and 1995 toward the ultracompact bipolar H II region NGC 7538 IRS1. We find, at both wavelengths, clear evidence of a decrease in the emission from the lobes. This decrease, of order 20-30%, has not been observed previously in any ultracompact H II region. Most likely, it is due to recombination of the ionized gas in the lobes as a result of a decrease in the available ionizing photon flux. It is unclear if this decrease in the ionizing photon flux is due to an intrinsic change in the exciting star or to increased absorption of ionizing photons in the optically-thick core of the nebula.

Subject headings: HII REGIONS — ISM: INDIVIDUAL (NGC 7538 IRS1) — STARS: PRE-MAIN-SEQUENCE

1. Introduction

The ultracompact H II (UC HII) regions are small (diameters $< 10^{17}$ cm) and dense (electron densities $> 10^4$ cm $^{-3}$) structures of gas that are maintained ionized by deeply embedded, recently formed O stars. They have a few recurring morphological types, one of them is the bipolar type that comprises only a handful of objects (Churchwell 2002). The bipolar UC HII regions have an hourglass shape when projected in the sky, the waist is believed to be produced by confinement by a disk or torus of neutral gas, while the lobes contain outflowing gas.

One of the most studied bipolar UC HII regions is NGC 7538 IRS1. It was first found in the infrared by Wynn-Williams, Becklin & Neugebauer (1974), and later its free-free emission was clearly resolved at centimeter wavelengths by Campbell (1984). Its radio spectrum

becomes fully optically thin only above ~ 100 GHz, with a total flux density of ~ 1.6 Jy at this frequency (Akabane et al. 1992). At a distance of 2.8 kpc (Sandell, Wright, & Forster 2003), this flux density implies an ionizing photon rate of $1.5 \times 10^{48} \text{ s}^{-1}$, that could be provided by an O8.5 ZAMS star with luminosity of $5 \times 10^4 L_{\odot}$ (Thompson 1984).

There is a large scale molecular outflow in the region (CO: Campbell & Thompson 1984; HCN⁺: Batrla, Pratap & Snyder 1988), that was proposed to be associated with NGC 7538 IRS1, but observations made by Batrla, Pratap & Snyder (1988) suggest that the source that is driving the outflow is located $\sim 15''$ south of IRS1. Gaume et al. (1995) made H66 α recombination line observations and found that this source has one of the most broad profiles ($\Delta v \simeq 150 \text{ km s}^{-1}$) seen in UC HII regions. There are also several masers associated with the source (e.g. OH: Hutawarakorn & Cohen, 2003; CH₃OH: Minier, Booth & Conway, 2000 ; H₂O: Kameya et al. 1990; ¹⁵NH₃: Gaume et al. 1991), among them there is the rare formaldehyde (H₂CO) 4.83 GHz maser (Hoffman et al. 2003). Observations in HCN, HCO⁺ (Pratap, Batrla & Snyder 1991) and CS (Kawabe et al. 1992) show the presence of denser material around the source; this can account for the confinement of the outflow seen in radio, especially in the south direction.

In this paper we present the analysis of archival VLA continuum observations of NGC 7538 IRS1 made with high angular resolution. The main goal of our study was to search for proper motions or time variability in this compact object. In §2 we describe the observations; in §3 we discuss them, and finally in §4 our main conclusions are given.

2. Observations

The archive observations of the NGC 7538 IRS1 region were made using the VLA of the NRAO¹ in the A configuration. The 2 cm observations were made in four epochs, while those at 6 cm were made in two epochs (see Table 1). The observations were made in both circular polarizations with an effective bandwidth of 100 MHz. The data were edited and calibrated following the standard VLA procedures and using the software package AIPS. After self-calibration we made cleaned images of the region with the ROBUST parameter of IMAGR set to 0, to optimize the compromise between angular resolution and sensitivity. The data at 2 cm was then cross-calibrated using the techniques developed by Masson (1986). After cross-calibration, we made images using as restoring beam the average beam of the images made at different epochs (see Table 1). These images were then subtracted to produce difference

¹NRAO is a facility of the National Science Foundation operated under cooperative agreement by Associated Universities, Inc.

images in order to search for small changes across time. We could not cross-calibrate the 6 cm data given the presence of bright, extended sources in the primary beam. These extended sources are not well described by the data (because it does not have short enough spacings), and since they dominate the total emission of the region, cross-calibration at 6 cm was not feasible.

The cross-calibration method of Masson (1986) tries to minimize differences, introduced by phase and amplitude errors, between the two epochs being compared. This tends to equalize the total flux density in the images being compared. However, even before cross-calibration, it was evident in our data that the southern lobe of NGC 7538 IRS1 was decreasing in flux density with time. We then introduced an additional criterion in the analysis of the data. Since the central region of the source is optically thick, we assumed that it did not change significantly with time and minimized its rms in the difference image, after the method of Martí, Rodríguez, & Reipurth (1998). For this, after cross-calibration, we subtracted the 2 cm images allowing one of them to have small shifts in position as well as a small scaling in its absolute amplitude value. Then, the difference image, ΔI , is given by

$$\Delta I = I_1(\alpha, \delta) - (1 + \epsilon)I_2(\alpha + \Delta\alpha, \delta + \Delta\delta),$$

where I_1 and I_2 are the images for epochs 1 and 2, α and δ are the celestial coordinates, $\Delta\alpha$ and $\Delta\delta$ the shifts introduced (of order a few milliarcseconds), and ϵ is the scaling correction (of order a few percent). In the case of the 6 cm images, cross-calibration was not feasible and the images were treated using only the last criterion.

3. Discussion

3.1. The Bipolar UC HII NGC 7538 IRS1

The 2 cm images of NGC 7538 IRS1 obtained for the three epochs shown in Fig. 1 are very similar among them and show the well-known bipolar morphology first seen by Rots et al. (1981) and Campbell (1984). The inner parts of the structure have a peak flux density of 26 mJy beam⁻¹ (average of the three epochs), that for a beam of 0''13, implies a brightness temperature of ~ 8400 K. Since we are observing free-free emission from photoionized gas with an electron temperature of this order, this result implies that these regions are optically thick. Observations made at 1.3 cm by Gaume et al. (1995) indicate clumpiness in this inner region and thus that the brightness temperature is even higher in some positions. We will assume an electron temperature of 10^4 K.

The inner two peaks of the source are at $\sim 0''.1$ from the center. At this position, we estimate the width of the structure to be also of order $\sim 0''.1$. At a distance of 2.8 kpc, an angular size of $0''.1$ corresponds to 1.4×10^{-3} pc. Since in the inner parts of NGC 7538 IRS1 the free-free opacity at 2 cm exceeds 1, $\tau_{2\text{ cm}} \geq 1$, this implies an emission measure $EM \geq 9.0 \times 10^8 \text{ cm}^{-6} \text{ pc}$. Assuming a physical depth of 1.4×10^{-3} pc for the emission region, we derive a lower limit for the electron density of $n_e \geq 8.0 \times 10^5 \text{ cm}^{-3}$.

The lobes of the structure are markedly asymmetric, with the northern one reaching peak flux density values of $\sim 6 \text{ mJy beam}^{-1}$, while the southern one reaches peak flux density values of $\sim 15 \text{ mJy beam}^{-1}$. Making similar assumptions that for the central regions, these flux densities imply that the lobes reach moderate optical depths, ($\tau_{2\text{ cm}} \simeq 0.2\text{-}0.4$), and electron densities in the order of $n_e \geq 4.0 \times 10^5 \text{ cm}^{-3}$. Similar conclusions about the morphology of NGC 7538 IRS1 were obtained by Campbell (1984).

The large electron densities of NGC 7538 IRS1 imply fast electron recombination times, $t_e \simeq 1/(n_e \alpha_B)$, where $\alpha_B = 2.6 \times 10^{-13} \text{ cm}^{-3} \text{ s}^{-1}$ is the recombination coefficient for $T_e = 10^4$ K. We then obtain recombination times of order 0.15 years for the core and 0.3 years for the lobes.

3.2. Difference Images

In Figure 1 we show the difference image for 1995.50-1983.89. The same features observed in this difference image are seen in the difference images for 1995.50-1986.18 and for 1986.18-1983.89 (not shown here) but, as expected, with less intensity given the smaller time difference.

The most clear feature of the 1995.50-1983.89 difference image is the large negative region appearing at the position of the southern lobe. Since the lobes have only moderate optical depths at 2 cm, we interpret this negative region as a decrease in the free-free emission. The decrease in flux density in the southern lobe between the two epochs is $\sim 30 \text{ mJy}$. This represents a large decrease, of $\sim 30\%$, in the flux density of the southern lobe that went from about 98 mJy in 1983.89 to 68 mJy in 1995.50. However, this large change in the lobe represents a relatively small change in the total flux density of the source. Since the total free-free flux density of NGC 7538 IRS1 at high frequencies is 1.6 Jy and assuming that it is divided equally between the two lobes, we conclude that this decrease represents a negative change of only $\sim 4\%$. Then, a relatively small change in the total ionizing photon flux of the region, produces a large relative change in the lobes. This is due to the fact that most of the ionizing photon flux is absorbed in the core region, with only the final $\sim 10\%$

being absorbed by the lobes. Then, a small change of a few percent in the total ionizing flux appears “amplified” in the lobes by a factor of ~ 10 .

There is also a negative region in the difference map associated with the northern lobe, implying a decrease of $\sim 20\%$ between 1983.89 and 1995.50, consistent with what is observed in the southern lobe. Despite our attempts to minimize the rms of the central regions (the “waist”) of the source, there are two positive regions of emission left whose nature remains uncertain.

To confirm this decrease in the emission of the radio lobes of NGC 7538 IRS, we made difference maps in a similar way for the 6 cm observations made in 1983.89 and 1995.65 (see Figure 2). Again, negative regions associated with the lobes appear in the difference map. This result is in a way surprising because the lobes can reach free-free optical depths in excess of 2 (and we should not be able to see through them). We tentatively attribute the variation to clumpiness in the lobes that could produce lines of sight with lower opacity.

Over approximately the same period of the continuum observations analyzed here, Hoffman et al. (2003) report a systematic *increase* in the emission of a bright 6 cm formaldehyde maser feature. It is unclear if this systematic trend in the maser emission is related with that observed in the continuum.

Finally, to check the reliability of our method we analyzed 2 cm images taken close in time, namely in 1995.50 and 1995.65. As expected given the very short time interval between observations, the difference image (Figure 3) does not show any significant residual structures (with the possible exception of a marginal negative feature in the southern lobe).

3.3. Possible Explanations for the Decrease in the Flux Density of the Lobes

What could be causing the decrease in flux density in the lobes of NGC 7538 IRS1? We start noting that, by several reasons, the decrease cannot be caused by proper motions of the ionized gas. First, proper motions of regions of emission appear in the difference image as a pair of features: one negative at the old position of the emitting region and located closer to the central star, and a positive one at the present position of the emitting region and located more distant from the central star (see, for example, Fig. 1 of Rodríguez et al. 2001). Furthermore, variations due to proper motions would imply displacements of order $0''.3$ (the width in the sky of the southern lobe) on a time scale of a few years (the decrease is evident even in the 1986.18-1983.89 difference image), that would translate in velocities of order $1,800 \text{ km s}^{-1}$, much larger than the velocities of $\sim 150 \text{ km s}^{-1}$ expected for the ionized outflow. Finally, the morphology of the lobes remains similar between epochs and

the decrease in flux density appears more or less simultaneously in an extended region.

The discussed characteristics of the flux density decrease suggest that, more likely, we are observing recombination of the ionized gas in the lobes due to a decrease in the available ionizing photon flux. As noted before, the recombination time of the ionized gas in the lobes is only ~ 0.3 years. We then favor as the explanation a decrease in the ionizing photon flux that reaches the lobes. This decrease could result from a decrease in the ionizing photon flux produced by the central star. However, from the evolutionary canonical models of Bernasconi & Maeder (1996), it can be shown that as a massive young star similar to that required to ionize NGC 7538 IRS1 settles into the main sequence, there are small changes in its ionizing photon flux of order 10%, but on timescales in the order of 5,000 years. Then, it appears that these intrinsic changes in the stellar ionizing photon flux cannot account for a 4% decrease in only ~ 11 years.

Another possibility is that the decrease observed in the lobes is due to increased absorption of ionizing photons in the core of NGC 7538 IRS1. For example, there could be increased injection of gas from the neutral torus into the surroundings of the central star, decreasing the amount of photons available for the lobes. Unfortunately, we cannot test this hypothesis directly given the large free-free opacity of the core at centimeter wavelengths. Future observations above 100 GHz (where all the nebula is expected to be optically thin in the free-free) could show that the *total* flux density of the region remains constant, with the lobes decreasing and the core increasing correspondingly. The presence in the difference 2 cm image of positive components in the core region (see Fig. 1) suggests that this hypothesis could be correct.

4. Conclusions

Our main conclusions can be summarized as follows.

1) We analyzed data taken at 2 cm toward the bipolar UC HII region NGC 7538 IRS1, finding that its lobes show a decrease in flux density in the order of 20-30% over a time interval of 11 years. The 6 cm data confirm this result.

2) This relatively large decrease in the emission from the lobes is tentatively interpreted as due to recombination of the ionized gas, caused by a decrease in the available ionizing photon flux.

3) At present it is unclear if this decrease in the ionizing photon flux of the lobes is due to an intrinsic change in the exciting star or to increased absorption of ionizing photons in

the core of the object.

RFH and LFR acknowledge the support of DGAPA, UNAM, and of CONACyT (México). This research has made use of the SIMBAD database, operated at CDS, Strasbourg, France.

REFERENCES

- Akabane, K., Tsunekawa, S., Inoue, M., Kawabe, R., Ohashi, N., Kameya, O., Ishiguro, M., & Sofue, Y. 1992, PASJ, 44, 421
- Batrla, W., Pratap, P. & Snyder, L. E. 1988, ApJ, 330, 67
- Bernasconi, P. A., & Maeder, A. 1996, A&A, 307, 829
- Campbell, B. 1984, ApJ, 282, L27
- Campbell, B. & Thompson, R. I. 1984, ApJ, 279, 650
- Churchwell, E. 2002, ARA&A, 40, 27
- Gaume, R. A., Johnston, K. J., Nguyen, H. A., Wilson, T. L., Dickel, H. R., Goss, W. M. & Wright, M. C. H. 1991, ApJ, 376, 608
- Gaume, R. A., Goss, W. M., Dickel, H. R., Wilson, T. L. & Johnston, K. J. 1995, ApJ, 438, 776
- Hoffman, I. M., Goss, W. M., Palmer, P. & Richards, A. M. S. 2003, ApJ, 598, 1061
- Hutawarakorn, B. & Cohen, R. J. 2003 MNRAS, 345, 175
- Kameya, O., Morita, K. I., Kawabe, R. & Ishiguro, M. 1990, ApJ, 355, 562
- Kawabe, R., Suzuki, M., Hirano, N., Akabane, K., Barsony, M., Najita, J. R., Kameya, O. & Ishiguro, M. 1992, PASJ, 44, 435
- Martí, J., Rodríguez, L. F., & Reipurth, B. 1998, ApJ, 502, 337
- Masson, C. R. 1986, ApJ, 302, L27
- Minier, V., Booth, R. S. & Conway, J. E. 2000, A&A, 362, 1093
- Pratap, P., Batrla, W., & Snyder, L. E. 1990, ApJ, 351, 530

Rodríguez, L. F., Torrelles, J. M., Anglada, G., & Martí, J. 2001, *RevMexA&A*, 37, 95

Rots, A. H., Dickel, H. R., Forster, J. R., & Goss, W. M. 1981, *ApJ*, 245, L15

Sandell, G., Wright, M., & Forster, J. R. *ApJ*, 590, L45

Thompson, R. I. 1984, *ApJ*, 283, 165

Wynn-Williams, C. G., Becklin, E. E. & Neugebauer, G. 1974, *ApJ*, 187, 473

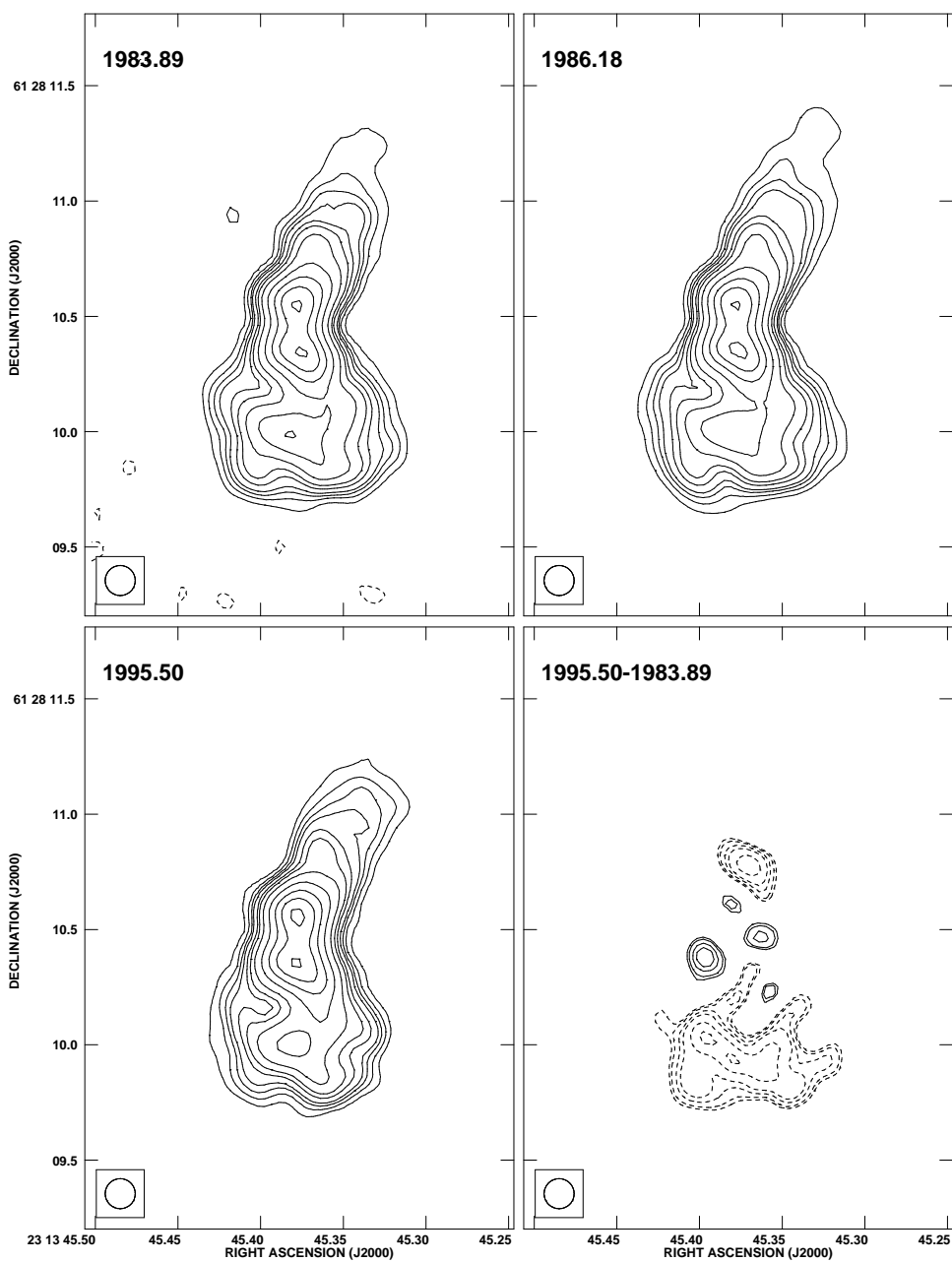


Fig. 1.— Images of NGC 7538 IRS1 at 2 cm for epochs 1983.89, 1986.18, and 1995.50, as well as the difference image for 1995.50-1983.89. All images are reconstructed with a circular Gaussian beam with HPBW of $0''.13$. The contours for the images of the individual epochs are -5, 5, 10, 15, 20, 30, 40, 60, 100, 150, 200, and 250 times $0.1 \text{ mJy beam}^{-1}$, the average rms of the three images. The contours for the difference image are -40, -30, -25, -20, -15, -10, -8, -6, -5, 5, 6, 8, 10, 15, and 20 times $0.2 \text{ mJy beam}^{-1}$.

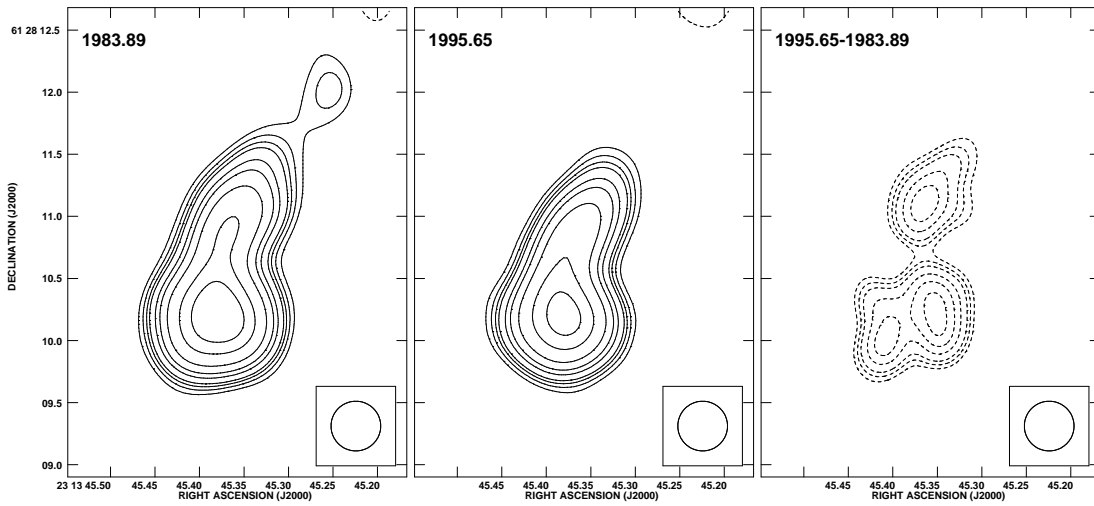


Fig. 2.— Images of NGC 7538 IRS1 at 6 cm for the epochs 1983.89 and 1995.65, as well as the difference image for 1995.65-1983.89. All images are reconstructed with a circular Gaussian beam with HPBW of $0''.4$. The contours for the images of the individual epochs are -4, 4, 6, 8, 10, 15, 20, 30, 50, 70, and 100 times $0.23 \text{ mJy beam}^{-1}$, the average rms of the two images. The contours for the difference image are -20, -15, -12, -10, -8, -6, -5, -4, 4, and 5 times $0.27 \text{ mJy beam}^{-1}$.

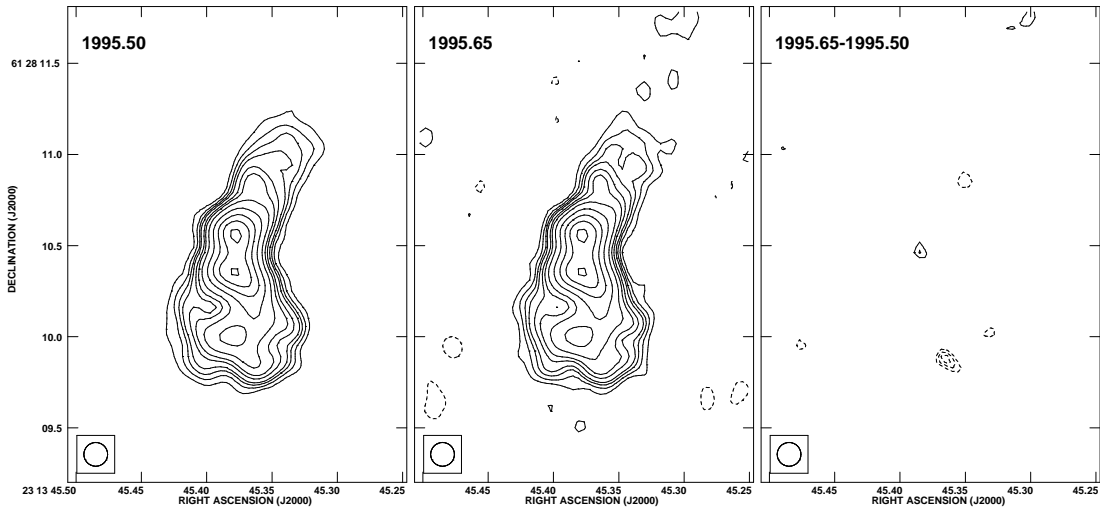


Fig. 3.— Images of NGC 7538 IRS1 at 2 cm for the epochs 1995.50 and 1995.65, as well as the difference image for 1995.65-1995.50. All images are reconstructed with a circular Gaussian beam with HPBW of $0''.13$. The contours for the images of the individual epochs are as in Figure 1. The contours for the difference image are -5, -4, -3, 3, 4, and 5 times $0.23 \text{ mJy beam}^{-1}$.

Table 1. Observational Parameters

Wavelength (cm)	Epoch	Amplitude Calibrator	Phase Calibrator	Bootstrapped Flux Density (Jy)	Beam ($'' \times '' ; ^\circ$)	rms noise (mJy)
2	1983 Nov 20	1331+305	2230+697	1.23 ± 0.03	$0.13 \times 0.12; +12$	0.18
2	1986 Mar 06	1331+305	2230+697	0.94 ± 0.01	$0.15 \times 0.11; +85$	0.07
2	1995 Jun 30	0137+331	2230+697	0.30 ± 0.01	$0.14 \times 0.12; -25$	0.12
2	1995 Aug 26	0137+331	0019+734	0.92 ± 0.02	$0.13 \times 0.11; -6$	0.21
6	1983 Nov 20	1331+305	2230+697	1.43 ± 0.01	$0.41 \times 0.38; -33$	0.22
6	1995 Aug 26	0137+331	0019+734	1.38 ± 0.01	$0.40 \times 0.37; +42$	0.26